Hydrodynamic entrapment of bacteria swimming near a solid surface

Davide Giacché,[1] Takuji Ishikawa,[1] and Takami Yamaguchi[2]
[1]*Department of Bioengineering and Robotics, Tohoku University, Sendai, Japan*
[2]*Department of Biomedical Engineering, Tohoku University, Sendai, Japan*

The near-surface motility of bacteria is important in the initial formation of biofilms and in many biomedical applications. The swimming motion of *Escherichia coli* near a solid surface is investigated both numerically and experimentally. A boundary element method is used to predict the hydrodynamic entrapment of *E. coli* bacteria, their trajectories, and the minimum separation of the cell from the surface. The numerical results show the existence of a stable swimming distance from the boundary that depends only on the shape of the cell body and the flagellum. The experimental validation of the numerical approach allows one to use the numerical method as a predictive tool to estimate with reasonable accuracy the near-wall motility of swimming bacteria of known geometry. The analysis of the numerical database demonstrated the existence of a correlation between the radius of curvature of the near-wall circular trajectory and the separation gap. Such correlation allows an indirect estimation of either of the two quantities by a direct measure of the other without prior knowledge of the cell geometry. This result may prove extremely important in those biomedical and technical applications in which the near-wall behavior of bacteria is of fundamental importance.

I. INTRODUCTION

The near-surface motility of microorganisms is important in the initial formation of biofilms as it influences the probability of adhesion of the cells to the surface. Biofilms can be found virtually anywhere: they are responsible for a wide variety of microbial infections in the human body, play a vital role in many natural phenomena, such as corrosion and biological fouling—the latter is particularly important for the hulls of ships—and their biomedical and technical applications have grown considerably in recent years [1–6]. Hence, the study of the near-wall motility of bacteria is not only a requisite for an enhanced understanding of the physical phenomenon, but can also potentially form the basis for controlling biofilm formation for bioengineering applications. In this context, the role of a reliable numerical tool to predict with a good level of accuracy the swimming behavior of bacteria could be significant, especially since a technique for growing filamentous cells of *Escherichia coli* with defined shapes has recently been developed [7].

The flagellate bacterium *E. coli* is particularly important because a large amount of information, gathered over the last three decades, is available for the construction of bacterial models, and experiments can be performed to validate the numerical approach. Precisely for these reasons, in the present study, a boundary element method has been used to investigate the near-wall motility of flagellated bacteria whose shape and swimming motion are directly referable to those of *E. coli*. The numerical approach to predict the trajectories and separation gap between the cell and the surface has also been validated by experiments conducted by the authors on *E. coli* of wild-type strain MG1655.

Escherichia coli is a peritrichous bacterium that swims in a random walk alternating essentially straight trajectories (runs) and rapid changes of direction while remaining in place (tumbling). In smooth forward motion, the flagella form a large bundle, and their concerted action propels the bacterium in a linear (in the time-averaged sense) "run" with speeds up to ten body lengths per second [8]. The presence of a solid boundary modifies significantly the characteristic smooth swimming motion of *E. coli* bacteria: the trajectories change from approximately straight in free swimming to circular in proximity to a planar wall. This circular motion (clockwise when seen from above) has been observed to remain stable often for long periods of time [9,10], and the physical mechanism underlying this rotation was explained in [10].

Three elements characterize the swimming motion near a planar solid surface: the radius of curvature of the trajectory, the swimming speed, and the minimum distance of the cell from the boundary. The radius of curvature for *E. coli* has been measured experimentally in several studies [10–14], and it is usually on the order of tens of micrometers (10–50 μm), but values up to 100 μm have also been observed [12]. Similar values were also observed for the singly flagellated marine bacterium *Vibrio alginolyticus* [15]. The swimming speed of *E. coli* near a solid surface has also been investigated experimentally and was found to be on the order of tens of μm/s [10,11].

The third—and perhaps the most difficult to measure—element characterizing the near-wall motility of swimming bacteria is the minimum separation distance between the cell and the surface. This quantity has been measured for motile *E. coli* using either three-dimensional tracking microscopy [11,12] or total internal reflection aqueous fluorescence microscopy [9]. The separation gap was found to span from 10 nm to a few hundred nanometers.

All the aforementioned three elements are a result of the hydrodynamic interaction of the bacterium with the surface and should be considered simultaneously. Previously, only two numerical studies have considered the near-wall hydrodynamics of bacteria [10,16]. In the first, Ramia *et al.* extended in [16] the pioneering work of Phan-Thien *et al.* [17] on a boundary integral method in Stokes flow regime to numerically predict the hydrodynamics of bacteria near a planar

solid surface under the simplifying assumption of spherical shape of the cell body with a single helical filament representing the flagellar bundle [8]. Their results replicated the experimentally observed circular trajectories of bacteria near a solid boundary, but did not (and could not give the computational resources available at the time) investigate the hydrodynamic trapping mechanism in detail.

More recently, Lauga *et al.* [10] developed a hydrodynamic model that employs resistive-force theory to calculate the trajectory of the bacteria again in the assumption of spherical cell body. The method is very powerful in explaining the physical picture and provides a reasonable agreement with experimental results. Furthermore, an analytical hydrodynamic model was derived as an approximation of the full model removing the need of numerical integration to obtain the cell trajectories. However, both the full model and its analytical approximation lack the capability of predicting the gap between the bacterium and the wall and do not include provisions for the hydrodynamic interaction between the cell body and the flagellar bundle.

As a last remark, it is important to observe that in both studies [10,16] the assumption of sphericity is questionable for two reasons: (1) for bacteria the size of the cell body is relatively large compared to the flagellar bundle; thus, it can be expected that the hydrodynamic trapping mechanism depends heavily on the shape of the cell body; and (2) the body of an *E. coli* cell is usually a prolate spheroid with an aspect ratio, short to long semiaxis, of 0.5.

Thus, the following fundamental questions still remain to be addressed: (a) Can the distance between a cell swimming near a solid surface and the surface itself be predicted numerically? (b) Is such a distance hydrodynamically stable? (c) Is this distance unique or are there multiple stable distances from the wall? (d) How do the cell geometry and initial position and orientation affect the swimming distance from the surface? (e) Is there a global correlation between the cell geometry and the swimming distance? (f) How accurate the numerical model is by comparing with the experiments?

To answer these questions, we investigate the hydrodynamic entrapment of bacteria near a solid surface using a boundary element method for typical bacterial geometries. Because the role of hydrodynamic forces has now been widely recognized in the entrapment of bacteria swimming near a solid surface as opposed to the electrostatic and van der Waals forces at the base of the Derjaguin-Landau-Verwey-Overbeek (DLVO) theory [9], only the former entrapment mechanism is considered here. In the following analysis, we show the existence of a stable hydrodynamic swimming distance, which depends on the shape of both the cell body and flagellum, and is independent on the cell's initial position and orientation. The numerical method is validated against experimental data collected for *E. coli* cells labeled with a fluorescent dye. A database is compiled for different bacterial geometries, and a correlation between the radius of the trajectory and the separation gap is derived. The analysis takes into consideration only smooth-swimming bacteria and does not model tumbling.
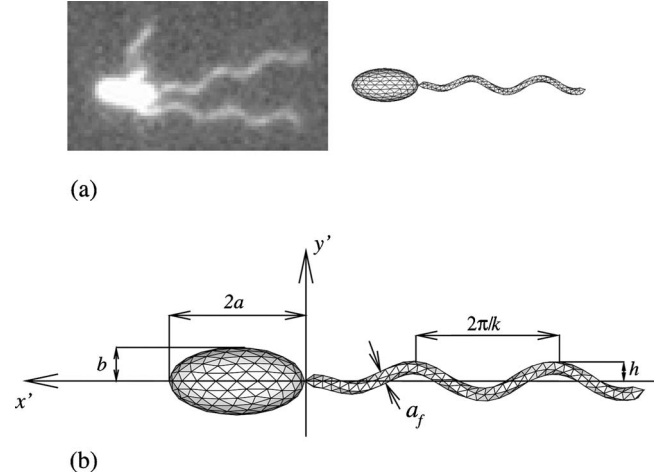

FIG. 1. Bacterial model: (a) photograph of a labeled *E. coli* cell (left) and corresponding computational model (right); (b) definition of the model's geometrical parameters and mesh.

II. BACTERIAL MODEL

The model employed in the current study is the same as that used in [18]. The bacterium is modeled as a single flagellar cell with an ellipsoidal (prolate spheroid) body with long semiaxis a, short semiaxis b, and aspect ratio (AR) $b/a < 1$ (see Fig. 1). The flagellum is assumed to be a cylindrical filament of cross-sectional radius a_f that executes helical waves according to the model of Higdon [19]. The flagellar waveform is prescribed, and the flagellum is assumed to rotate (rigidly) with constant angular velocity ω relative to the cell body. The overall length of the flagellum, L, is computed as a line integral along the helix.

The present model applies not only to real bacteria with a spheroidal body and a single helical flagellum such as the eubacteria *Photobacterium phosphoreum* and *Pseudomonas aeruginosa*, but also to peritrichous bacteria like *E. coli* in forward smooth-swimming motion when the flagella rotate as a tight bundle and effectively act as a single propulsive unit. This simplification is supported by the observation that the external hydrodynamic differences between a flagellar bundle and a single flagellum should not be significant [8].

The bacterium is assumed to be neutrally buoyant in virtue of the typical much smaller than unity ratio between the sedimentation and swimming speed, and the center of buoyancy is assumed to coincide with the geometrical center of the cell, so that the model is torque- and force-free. Brownian motion is not considered in the present study because we did not observe any large fluctuations in the near-wall trajectories of *E. coli* bacteria in our experiments.

A boundary element method is used to study the hydrodynamic interaction in Stokes flow regime [18,20]. Half-space Green's function [21] is introduced to express the effect of a solid wall (for details, refer to supplementary material S1 [22]). The cell body is discretized with 320 triangular elements, whereas the flagellum is modeled as a series of pentagonal cylinders whose surface is composed of 360 triangular elements (see Fig. 1). The kinematic constraint at the junction between the body and the flagellum is

satisfied by using a pentagonal pyramid to represent the first segment of the flagellum; a similar treatment is used at the end of the flagellum [17,18].

All physical quantities have been nondimensionalized with the cell body long semiaxis a[m], the fluid viscosity μ[Pa s], and the angular velocity ω[rad s^{-1}]. Typical values for an *E. coli* bacterium are approximately 3 μm for the body length $2a$, a cell body aspect ratio of 0.5, a flagellum length of ~7 μm, and 100–1000 s^{-1} for the angular velocity [8,13].

III. EXPERIMENTAL MATERIALS AND METHODS

A. Preparation of motile cells

Saturated *Escherichia coli* cultures (wild-type MG1655, National Institute of Genetics, Japan) were grown for 12 h in tryptone broth (TB) culture fluid [tryptone 1.2% (w/v), yeast extract 2.4% (w/v), and glycerol 0.4% (v/v)] kept at 37 °C using a rotary shaker (160 rpm). A sample of 50 μl of the saturated culture was then diluted in 5 ml of TB culture fluid and kept at 25 °C without shaking for 10 h. *E. coli* cells were labeled by Cy3 monofunctional succinimidyl ester (PA23001, American Pharmacia Biotech, Newark, NJ, USA) according to the labeling protocol reported in [23]. The labeled motile *E. coli* bacteria were finally suspended with motility buffer MB+ (0.01 M potassium phosphate, 0.067 M NaCl, 10–4 M EDTA; pH 7.0) containing 0.002% Tween 20 (Sigma-Aldrich, St. Louis, MO, USA) and 0.5% glucose. The number density of cells was adjusted to less than 10^8 cells/ml, which is too small for cell-cell interactions to be important.

B. Experimental setup

The experimental setup was designed to measure the trajectories of cells near a glass wall. Bacteria were observed at room temperature (23 °C) with an upright microscope (Leica DM4000B, Solms, Germany) with an objective lens (Leica 506197, 100×/1.30 Oil PH3, Solms, Germany). Video images were acquired using a charge-coupled device camera (Leica DFC340FX, Solms, Germany) connected to a digital video recorder that captured 800×600 pixel images at 30 frames per second. Illumination was provided by a mercury vapor short-arc lamp (ebq 100 mc-L, LEJ, Denmark). A volume of 190 μl of the labeled motile bacteria suspension was placed between a glass coverslip and a glass microscope slide. The coverslip was placed carefully to eliminate air bubbles and to form a chamber about 100 μm thick.

C. Video analysis

Video images were analyzed using TRACKER (available for download in [24]), which allows for automatic tracking of bacteria by capturing a mask image of a user-specified cell and searching each frame for the best match. The trajectory analysis involved fitting an ellipse using a least-squares method through the raw data and subsequently calculating the radius as the average distance from the center of the ellipse. Throughout the swimming motion of the bacterium,
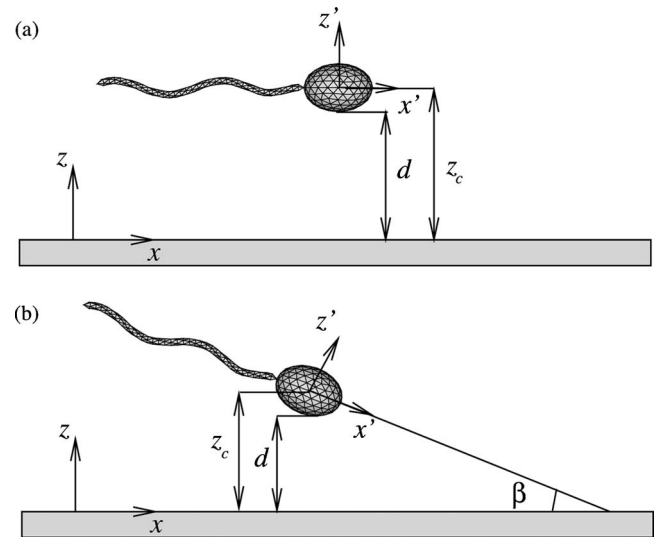

FIG. 2. Schematic illustration of the microorganism's initial position and orientation with respect to the solid surface: (a) initial orientation parallel to the wall; (b) generic initial orientation at an angle β.

the traces to be analyzed are determined using two criteria: (1) at the intersection point the angle between the tangents at the beginning and at the end of the closed curve must be $\leq 30°$ and (2) the Euclidean distance between the first point of the closed curve and the point after the intersection at the end of the trajectory should be ≤ 3 μm.

IV. RESULTS AND DISCUSSION

A. Stable swimming distance from the wall: Effect of initial position

The first question to address in the investigation of bacterial swimming near a solid boundary is whether for a given cell geometry only one stable time-averaged swimming distance from the surface exists or whether multiple stable distances can be observed depending on the initial position and/or orientation of the organism. Initially, the analysis focused on a bacterium model whose initial orientation vector lays on a plane parallel to the solid surface as depicted in Fig. 2(a). This choice is dictated by the fact that in this configuration no external repulsive force is required to prevent a collision between the cell and the surface from occurring due to numerical inaccuracy. This ensures that the entrapment mechanism predicted by the numerical method is exclusively hydrodynamic in nature.

The coordinates fixed to the solid planar boundary are designated as (x, y, z), with the z axis directed normal to the wall, located at $z=0$, and pointing toward the fluid ($z>0$); the origin of the coordinates system moving with the cell (x', y', z') is the center of the cell body and the x' axis coincides with the geometrical axis of the bacterium as depicted in Fig. 2. In order to study the effect of the cell's initial position on the time-averaged swimming distance from the wall, the location of the center of the cell body with respect to the solid boundary, z_c, is varied so that the mini-

TABLE I. Flagellar geometry parameters. k is the flagellar wave number, k_E is a constant that determines how quickly the helix grows to its maximum amplitude, a_f is the flagellar diameter, and h is the amplitude of the flagellar helix.

L	k	k_E	a_f	h
7	1.3	1.3	0.1	0.2

mum separation gap between the cell and the wall, d_{min}, ranges from 0.2 to 3.0 body lengths. Several bacterial models with different cell body aspect ratios but identical flagellar geometries are considered. The results for two models with cell body aspect ratios, respectively, of 0.5 and 0.7 are presented here. We will refer to the former model as *model A*, and to the latter as *model B*. The geometrical characteristics of the flagellum for both cases are summarized in Table I.

The results shown in Fig. 3 reveal that a stable swimming distance and its associated radius of curvature exist for each bacterial model, and that these do not depend on the initial position. It is also interesting to observe that in all the cases presented above, the cell swims at an angle to the wall of approximately $1°-2°$ with the x' axis pointing away from the surface. The existence of a stable swimming height (in the time-averaged sense) that depends only on the geometry of the bacterium is a result of fundamental importance for two reasons: (1) it provides the opportunity to predict such distance when the geometry of the bacterium is known irrespective of its initial position and (2) it may allow one to establish a simple correlation between the radius of curvature and the separation gap that could be used to indirectly estimate quantity from the experimental observation of the other (for example, the distance of a smooth-swimming bacterium in the vicinity of a wall—difficult to measure directly with
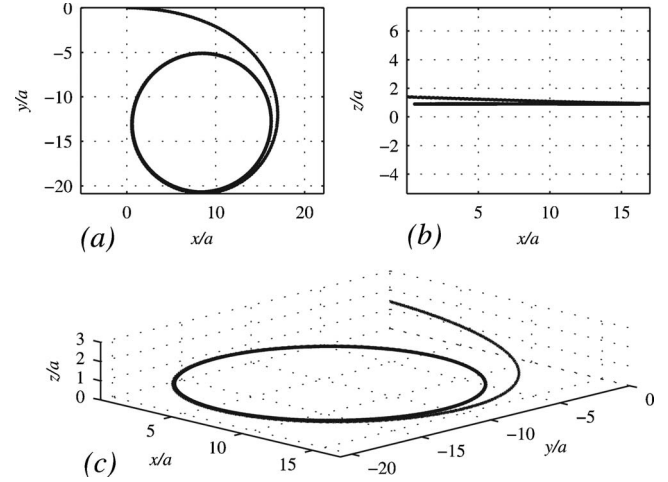
FIG. 4. Trajectory of bacterial model B: (a) x-y projection, (b) x-z projection, and (c) top-down perspective.

sufficient accuracy—could be determined by measuring the radius of curvature, which is relatively easy to evaluate).

As a last remark, it is important to observe that the bacteria trace only nearly circular trajectories; in fact they are elliptical with a ratio of the short and long semiaxes generally close to 1, as illustrated by the projection of the trajectory for model B on the x-y plane in Fig. 4. For a prescribed flagellar geometry, the trajectory becomes increasingly elliptical as the cell body aspect ratio departs from unity (see Tables S1–S3 of supplementary material [22]). This poses the question of how to compare different trajectories. In the current study, the quantity used in the comparison of elliptical trajectories is the mean distance from the center of the ellipse which corresponds to the radius of curvature of the trajectory when this is perfectly circular. For commodity, we will continue to refer to this distance as the "radius" of the trajectory in the remainder of this paper.

In the present example, the trajectories' semiaxis ratios are 0.90 and 0.98 for models A and B, respectively, and the predicted radii studied are approximately $26.3a$ and $7.8a$, in line with values observed experimentally [11,12]. In the framework of our numerical simulations, circular swimming could go on *ad infinitum* for a bacterium in isolation. In reality, for example, in the case of *E. coli*, tumbling or cell-cell interactions may interfere and disrupt the circular motion; in the absence of these perturbing factors *E. coli* can be observed swimming in circles near a wall for very long periods of time. This confirms that the method is fundamentally capable of capturing the physics of the phenomenon.

B. Effect of initial orientation

In order to generalize the results presented in the previous section, the influence of the initial orientation must also be addressed. A preliminary study for model A revealed that to avoid a "numerical" collision of the bacterium against the wall, an additional nonhydrodynamic repulsive force between the surface and the cell is required whenever the initial orientation vector forms an angle greater than 4° (vector pointing toward the surface). As mentioned in the previous
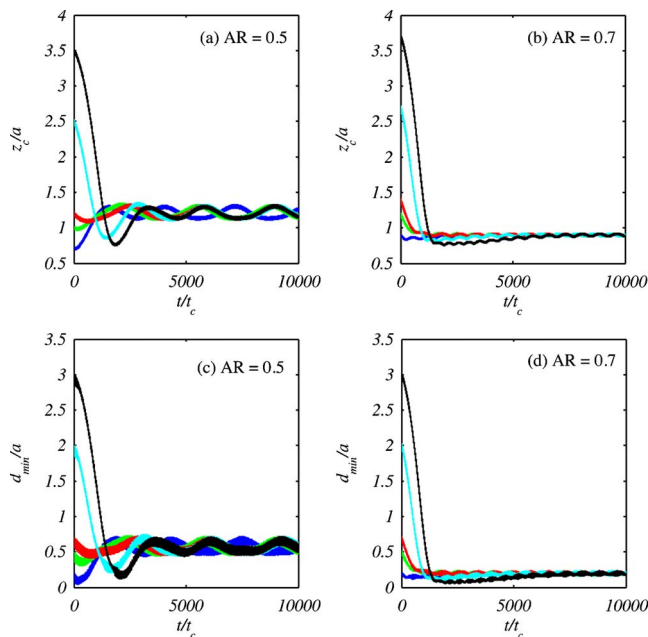

FIG. 3. (Color online) Minimum separation gap d_{min} and cell body center position z_c at the variation of the initial positions of models A and B: (a) and (c) model A; (b) and (d) model B.

section, this collision occurs because of numerical inaccuracy and not because of the physics of the Stokes flow.

In reality, an electrochemical force may exist between the bacterium and the surface, and for sufficiently small gaps this force may play a role in the cell-surface interaction. This type of force can be repulsive or attractive depending on the charge of the two objects, their distance, and the properties of the surrounding medium [12]. It is therefore plausible to include in our numerical model—which by its nature can only predict purely hydrodynamic phenomena—a short-range repulsive force [25] to deal with bacteria approaching the surface with large inclination angles (cf. supplementary material S2 [22]).

It is important to point out that a short-range repulsive force is utilized here merely to investigate whether one or multiple stable swimming hydrodynamic heights exist. The repulsive force only acts for a short period of time at the first "contact" of the cell with the surface and is otherwise of negligible magnitude with no bearing on the subsequent stable swimming motion.

In order to determine the effects of the initial orientation and the repulsive force on the stable swimming distance, a parametric study is carried out for several configurations with an inclination angle $\beta \geq 10°$. The center of mass of the bacterium is initially placed two body lengths away from the wall. The initial inclination angle formed between the axis of the bacterium and the solid surface, β, is varied from 10° to 60°: in particular, the values of 10°, 20°, 30°, 45°, and 60° are used. For each value of β, the range and magnitude of the repulsive force are varied, yielding two test cases per configuration.

The simulation results, shown in Figs. S1–S5 of supplementary material [22], indeed confirmed that a stable hydrodynamic distance exists, and that it does not depend on either the initial orientation or the repulsive force. Of course, the transient phase depends on the details of the repulsive force (see supplementary material S2 [22]). An important consequence of this result is that to determine the swimming height and radius of a given bacterial model it is sufficient to analyze the configuration with the initial orientation parallel to the wall without any artificially imposed repulsive force.

C. Comparison with experiments

Experimental measurements of the trajectories of individual *E. coli* bacteria labeled with a fluorescent dye in a dilute suspension have been used to validate the numerical method. Besides the measurement of the radius of the trajectory of cells swimming near the glass boundaries, an essential element of the validation is the determination of the cell geometrical features. The experimental setup allows one to measure easily the trajectories of single cells, but the accurate assessment of the cell geometry is laborious. Whereas the cell body aspect ratio and the length of the flagellar bundle can be determined with reasonable accuracy during the swimming motion, the clear determination of the flagellar geometry is only possible by manually tracking a cell throughout its motion until this adheres to the glass surface; at that point a picture of its individual flagella can be taken and the flagellar geometry can be determined.
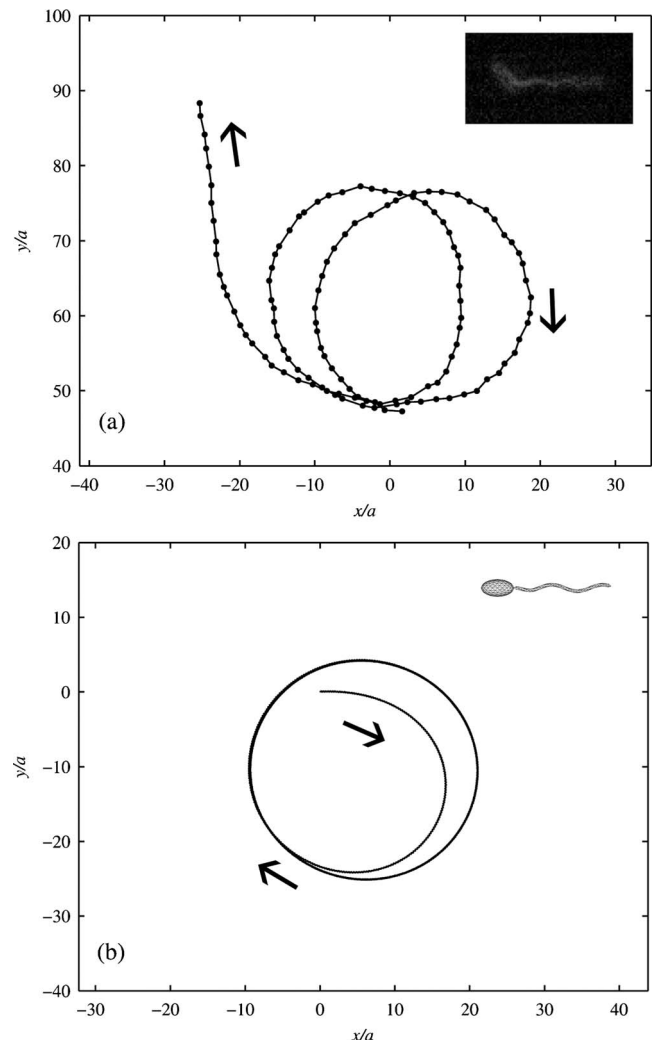

FIG. 5. Comparison between (a) measured traces generated by tracking individual *E. coli* cells and (b) predicted trajectories for a bacterium model with aspect ratio equal to 0.53, $L=6a$, and $k=1.3$ (see Table I for other flagellar parameters).

The chamber containing the test fluid is examined from above; hence the cells are observed swimming in a counter-clockwise direction when viewed from outside the chamber (upper wall) and in a clockwise direction when viewed from within the fluid (lower wall). Similarly to the numerical analysis results, the trajectories traced by the *E. coli* cells are found to be ellipses with small eccentricities, and an example of the raw trace obtained by video analysis is shown in Fig. 5(a). In order to perform the numerical simulation on a model with the same geometry of the real organism, the computational model of the swimming bacterium is reconstructed from individual snapshots of the *E. coli* cell as shown in Fig. 5(a). The trajectory of the computational model is shown in Fig. 5(b). The agreement between the two sets of results is remarkably good, and it exemplifies the level of agreement obtained for those bacteria of which the geometry could be clearly identified.

Cells seldom trace one trajectory over and over again in time because many external factors can interfere, e.g., inter-action with other cells, tumbling, asymmetry of the cell body
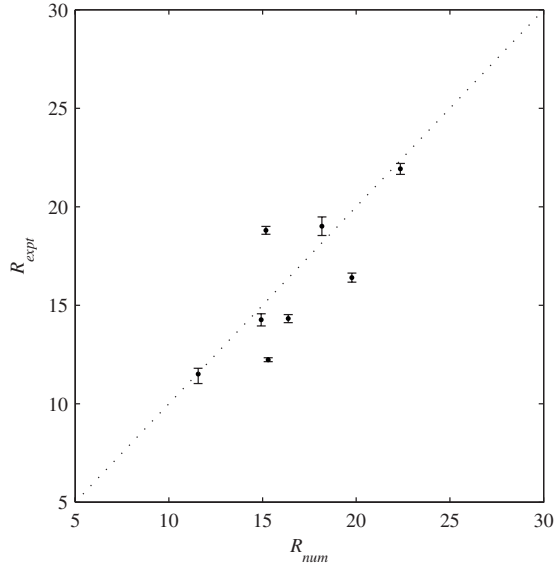
FIG. 6. Comparison between experimental measurements and numerical predictions of the radius of the trajectory.

FIG. 7. Correlation between separation gap and radius of trajectory: (a) $C_1=0.0951$, $C_2=0.0144$, $r^2=0.85$; (b) $C_1=0.1601$, $C_2=0.0070$, $r^2=0.77$; (c) $C_1=0.1253$, $C_2=0.0057$, $r^2=0.73$; and (d) $C_1=0.1142$, $C_2=0.0095$, $r^2=0.56$.

or of the flagellar bundle, etc. For this reason, instead of computing the radius of curvature on the base of partial curved traces in the assumption of circular trajectories as previously done in [10], an average of the mean radius is computed over the number of closed trajectories traced during the observation period that satisfy the criteria presented in Sec. III. The mean value of the radius thus obtained is compared to the numerical prediction, and the results are presented in Fig. 6. The error bars in R_{expt} show the minimum and maximum values of the radius measured for a given cell. Overall, the results shown in Fig. 6 demonstrate a good agreement between the numerical predictions and the experimental observations and contribute to validating the numerical method.

D. Parametric study: Radius-gap correlation

A parametric study has been carried out for the main geometrical features of our bacterial model: the flagellum length, the flagellar wave number, and the cell body aspect ratio. This study serves two purposes: first, to compile a database of the trajectory radii and separation gaps for typical bacterial geometries that can be consulted by scientists (see Tables S1–S3 of supplementary material [22]); and, second, to establish a correlation between the radius and the separation gap which could be used to estimate either of the two quantities when only one is known—for example, the separation gap could be estimated when only the radius of the trajectory is known from either experimental or numerical observations. A key advantage of using such a correlation is that, by sacrificing some accuracy, no prior knowledge of the bacterium geometry is required.

The length of the flagellum, its wave number, and the aspect ratio of the cell body are varied to cover a wide range of geometries. The flagellum length assumes the values of 6, 7, 8, and 9 unit lengths; the wave number is taken to be 1.3, 2, and 3; the cell body aspect ratio varies from 0.4 to 0.7 in
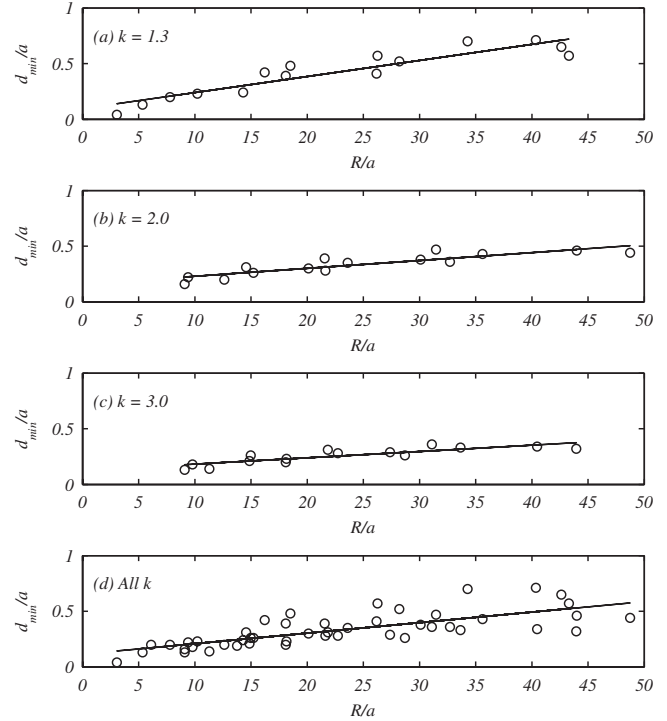
0.1 increments. All the remaining geometrical parameters are summarized in Table I.

The predicted values of the radius and separation distance for all the cases considered are shown in Fig. 7. The results are organized in Figs. 7(a)–7(c) according to the flagellar wave number, whereas Fig. 7(d) includes all the results and no geometrical information can be inferred from it. In each case, the relationship between the minimum distance from the surface and the radius is modeled using a linear regression model of the form $d_{\min}/a=C_1+C_2R/a$.

For all the cases presented in Fig. 7, the correlation between the minimum distance from the surface and the radius of the trajectory is strong. Perhaps, not surprisingly, the coefficient of determination r^2 is lower when no information about the flagellar wave number is known [Fig. 7(d)]. In this case, the value of r^2 is 0.56, which means that 56% of the total variation in the separation gap can be explained by the linear relationship as described by the regression equation. This seems to be a reasonable estimate when the shape of the bacterium is unknown.

E. Effect of stresslet

If we analyze the flow field of a cell swimming near a wall with the mathematical tool of flow singularities, we can describe the cell as a dipole [26–28]. In this case, the flow field can be derived as the linear superposition of the infinite fluid flow plus an image flow field on the opposite side of the wall. Following this kind of analysis, it can be demonstrated that the wall induces a rotation on the cell so as to align it

with the wall proportional to the strength of the dipole and inversely proportional to the cube of the distance from the wall [27,28]. Besides, the bacterium would be attracted to the surface with a speed scaling with the strength of the dipole and inversely proportional to the square of the distance. This type of analysis is strictly correct only when the bacterium is far away from the surface; nonetheless, it could prove important in defining a preliminary crude measure of the factors influencing the stable swimming height.

The strength of the dipole is proportional to the symmetric part of the hydrodynamic stress tensor (stresslet **S**) component in the swimming direction **e**, S_{ee} (cf. supplementary material S1 [22]), and it is ultimately determined by the geometry of the cell. Therefore, with this type of approach, we can establish a qualitative relationship between the geometry of the bacterium and the strength of the attraction to the wall. When no collision occurs, this attraction is balanced by a repulsive force of hydrodynamic nature, electrochemical, or indeed a combination. This balance determines the height at which the bacterium swims. The difficulty in establishing an analytical expression for the hydrodynamic repulsive force does not allow one to predict analytically the separation gap from the surface, but we can presume that this will reduce for increasing $|S_{ee}|$.

In order to test the validity of this argument, the stresslet component in the swimming direction has been calculated for all the bacterial models analyzed in the parametric study previously presented. The variation of the trajectory radius with $|S_{ee}|$ is shown in Fig. 8. Since the arguments used above are only strictly valid in the far-field approximation, we can only expect a reasonable agreement, but the results shown in Fig. 8 confirm the goodness of the "stresslet argument." A close examination of Fig. 8 also reveals how the stresslet and the radius vary with the geometrical parameters, and in particular how the radius generally reduces for increasing cell body aspect ratio, and with increasing flagellar length.

V. CONCLUSIONS

We have presented a numerical method to predict the near-wall motion of flagellated bacteria and compared it to a set of measurements of *Escherichia coli* cell geometries and trajectories. A good agreement between the numerical predictions and the experimental data was found, paving the way to the use of the numerical approach as a predictive tool when the cell geometry is known (at least partially).

In agreement with a far-field flow singularity argument, we showed an important qualitative relationship between the stresslet component in the direction of motion and the radius or the separation gap. In particular, we found that for a given flagellar wave number the bacterium tends to swim closer to the surface (tracing trajectories with smaller radii) with increasing cell body aspect ratio and with decreasing flagellar length.
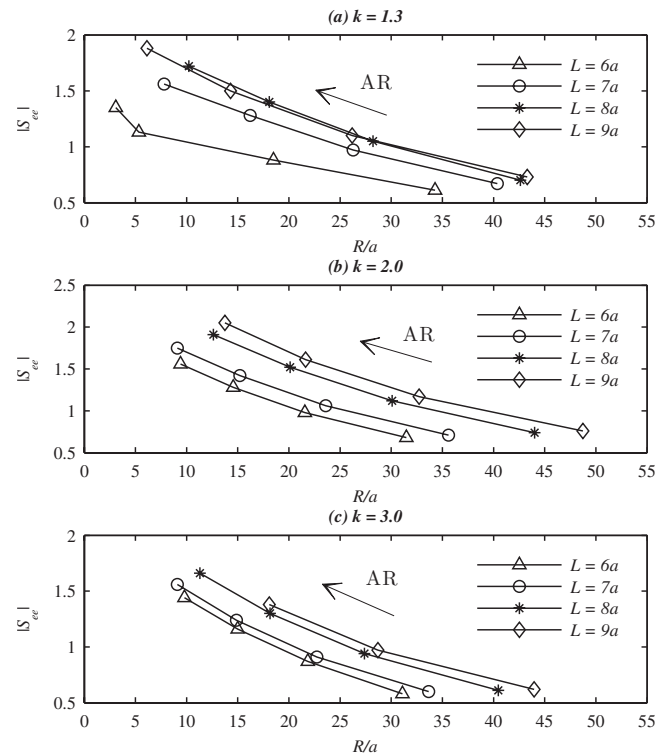

FIG. 8. Correlation between $|S_{ee}|$ and the radius of the trajectory: (a) $k=1.3$, (b) $k=2.0$, and (c) $k=3.0$. Information about the cell body aspect ratio (AR) and flagellum length L can also be read from the plots.

A database of solutions was compiled, and we demonstrated a strong linear relationship between the radius of the trajectory and the minimum distance of a swimming cell from the solid surface. The correlation allows an indirect estimation of either of the two quantities by a direct measure of the other without (or little) prior knowledge of the cell geometry. This result would be of interest to a large number of scientists developing biomedical and technical applications involving near-wall bacterial swimming, in addition to the possibility of using a numerical tool to investigate surface-cell adhesion and interaction processes. Examples include—but are not limited to—the analysis of the early formation of bacterial biofilms in newly developed polymeric implants, biofouling, water and wastewater treatment, and microfluidic biosensors.

[1] J. F. Lynch, H. M. Lappin-Scott, and J. W. Costerton, *Microbial Biofilms* (Cambridge University Press, Cambridge, England, 2003).

[2] R. Kolter and E. P. Greenberg, Nature (London) **441**, 300 (2006).

[3] J. J. Heijnen, M. C. M. van Loosdrecht, R. Mulder, R. Weltevrede, and A. Mulder, Water Sci. Technol. **27**, 253 (1993).

[4] C. A. Fux, J. W. Costerton, P. S. Stewart, and P. Stoodley, Trends Microbiol. **13**, 34 (2005).

[5] W. G. Characklis, M. J. Nevimons, and B. F. Picologlou, Heat Transfer Eng. **3**, 23 (1981).

[6] V. A. P. Martins *et al.*, *Microbial Biodegradation: Genomics and Molecular Biology* (Caister Academic Press, Norfolk, UK, 2008), pp. 269–296.

[7] S. Takeuchi, W. R. DiLuzio, D. B. Weibel, and G. M. Whitesides, Nano Lett. **5**, 1819 (2005).

[8] C. Brennen and H. Winet, Annu. Rev. Fluid Mech. **9**, 339 (1977).

[9] M. A. S. Vigeant, R. M. Ford, M. Wagner, and L. K. Tamm, Appl. Environ. Microbiol. **68**, 2794 (2002).

[10] E. Lauga, W. R. DiLuzio, G. M. Whitesides, and H. Stone, Biophys. J. **90**, 400 (2006).

[11] P. D. Frymier, R. M. Ford, H. C. Berg, and P. T. Cummings, Proc. Natl. Acad. Sci. U.S.A. **92**, 6195 (1995).

[12] M. A. S. Vigeant and R. M. Ford, Appl. Environ. Microbiol. **63**, 3474 (1997) [http://aem.asm.org/cgi/content/short/63/9/3474].

[13] H. C. Berg, *Escherichia coli in Motion* (Springer-Verlag, New York, 2004).

[14] R. M. Macnab, Proc. Natl. Acad. Sci. U.S.A. **74**, 221 (1977).

[15] T. Goto, K. Nakata, K. Baba, M. Nishimura, and Y. Magariyama, Biophys. J. **89**, 3771 (2005).

[16] M. Ramia, D. L. Tullock, and N. Phan-Thien, Biophys. J. **65**, 755 (1993).

[17] N. Phan-Thien, T. Tran-Cong, and M. Ramia, J. Fluid Mech. **184**, 533 (1987).

[18] T. Ishikawa, G. Sekiya, Y. Imai, and T. Yamaguchi, Biophys. J. **93**, 2217 (2007).

[19] J. J. L. Higdon, J. Fluid Mech. **94**, 331 (1979).

[20] T. Ishikawa, M. P. Simmonds, and T. Pedley, J. Fluid Mech. **568**, 119 (2006).

[21] J. R. Blake and A. T. Chwang, J. Eng. Math. **8**, 23 (1974).

[22] See supplementary material at http://link.aps.org/supplemental/10.1103/PhysRevE.82.056309

[23] N. C. Darnton, L. Turner, S. Rojevsky, and H. C. Berg, J. Bacteriol. **189**, 1756 (2007).

[24] http://www.cabrillo.edu/~dbrown/tracker/

[25] T. Ishikawa and T. J. Pedley, J. Fluid Mech. **588**, 399 (2007).

[26] T. Ishikawa, J. R. Soc., Interface **6**, 815 (2009).

[27] E. Lauga and T. R. Powers, Rep. Prog. Phys. **72**, 096601 (2009).

[28] W. R. DiLuzio *et al.*, Nature (London) **435**, 1271 (2005).